Surface reflections and optical transport through random media: Coherent backscattering, optical memory effect, frequency, and dynamical correlations

Isaac Freund and Richard Berkovits
Department of Physics, Bar-Ilan University, Ramat-Gan, Israel
(Received 17 July 1989)

The effects of internal surface reflections on the transport of optical waves through random media are considered theoretically. Simple closed-form expressions for both transmission through and reflection from a finite slab are obtained for the following phenomena: the coherent backscattering of light, the form factors of the optical memory effect, the frequency-dependent correlation functions of static systems, the time-dependent correlation functions of dynamic systems, and the diffuse reflectance and transmittance. In every instance surface reflections are found to cause significant, sometimes dominant, effects under realistic experimental conditions. Good agreement is found between the theory and recent experiments for the optical memory effect.

I. INTRODUCTION

Light injected into a highly random medium is considered to undergo a random walk due to strong multiple scattering. As a result of the discontinuity in refractive index (impedance mismatch) at the sample surface, light that attempts to exit through the surface may be internally reflected. This reinjection of the light can lead to a drastic lengthening of the random walk inside the medium, and thus to dramatic changes in properties which depend upon the length of the optical path and its associated distribution function. Surprisingly, perhaps, the randomness of the medium can greatly *enhance* the effective surface reflectivity. Because of the strong multiple scattering that destroys the directionality of the incident beam, all exit angles have approximately equal probability, so that a major fraction of the light attempts to exit at angles greater than the critical angle for the total internal reflection, θ_c. This fraction may be easily seen to equal $\cos\theta_c$. For a refractive index of 1.5, the effective reflectivity against air can approach 75% if the surface becomes highly reflecting at near grazing incidence, as is often the case. With such a large reflectivity, internal surface reflections become a dominant factor, and these reflections have very recently been shown experimentally[1] to have a dramatic influence upon the form factors of the optical memory effect[2-4] for both transmission and reflection. Since the form factor in reflection is closely related to the shape function of the coherent backscattering peak,[1] most of the experimental results[5-11] for this latter quantity are expected to have been significantly affected by surface reflections. This is also the case for other optical properties of current interest, such as the frequency-dependent correlation functions for static systems,[12-15] and the time-dependent correlation functions for dynamic systems.[16-25] Thus, it is clear that almost all of the recent experiments involving optical transport through highly random media (Refs. 1, 3, 5-12, 16-18, 20-22 and 24) are affected to a greater or lesser extent by internal reflections at the boundaries of the sample. Accordingly, any theory that neglects this important effect will necessarily be incomplete, while its use in the interpretation of experimental data may lead to significant errors.

The only prior theoretical treatment of these internal reflections is a very recent, important paper by Lagendijk, Vreeker, and De Vries[26] that treats the coherent backscattering peak and also pulse propagation. These authors develop a formulation for the Green's function that describes diffusive propagation of light in the presence of surface reflections. Although of intrinsic theoretical interest, there are two problems with such an approach. The first is the practical one that all the various phenomena described would now need to be recalculated using this new Green's function. The second problem is one of principle. The boundary conditions for the diffusion equation are a vexing problem that is usually resolved by fitting the diffusion equation solutions to the solution of the Milne equation.[27] But the Milne equation solutions are also altered (in a presently unknown fashion) by the reflectivities of the sample surfaces. Accordingly, there still exists a significant, presently unresolved uncertainty in the direct application of the diffusion equation to samples with surfaces of arbitrary reflectivity.

In contrast to this, we bypass the direct use of the diffusion equation, and for each process we provide a solution to the problem of surface reflections in terms of the already known solutions that exist in the absence of these reflections. As becomes apparent, such an approach is possible because successive passes of the light through the medium are statistically independent, so that the effects of surface reflections may be treated as simple reinjections of the emergent light. In this way we are able to obtain closed-form results for the coherent backscattering from a slab of finite thickness, something that had not proven possible using the Green's-function approach.[26] In a similar fashion, we also obtain simple closed-form expressions for a finite-thickness slab for the form factors of the optical memory effect, for the

frequency-dependent correlation functions of static systems, for the time-dependent correlation functions of dynamic systems, and for the diffuse reflectance and transmittance. The only case involving surface reflections in which suitable quantitative experimental data are currently available is the optical memory effect.[1] Accordingly, we compare our theoretical results with these experiments and find good agreement between theory and experiment both in reflection and in transmission. Since internal surface reflections play a dominant role in these experiments, we believe that the good agreement between theory and experiment provides a significant verification of our theoretical results, and suggests that these may be used with some confidence in a variety of realistic situations.

II. THEORY

Although it is possible to treat the general case of a finite-thickness slab directly, and from this derive all special cases, we start by considering a slab of infinite thickness with one boundary. This permits us to develop the rationale behind our treatment of the various phenomena in a simple, transparent fashion and to display in each case the essential effects of the surface reflections. Following this, the more complicated generalization to the finite-thickness slab with two (different) partially reflecting boundaries is carried out.

A. One boundary — coherent backscattering

We begin with the coherent-backscattering peak from a nonabsorbing, infinite half-space with one partially reflecting boundary. For normal incidence, the shape function for this peak, $\gamma(\mathbf{q})$ may be written

$$\gamma(\mathbf{q})=\int e^{i\mathbf{q}\cdot\mathbf{x}}P(\mathbf{x})d^2x \ , \tag{1}$$

where $q=k\sin\theta$ is the component of the scattered wave vector k, which is parallel to the boundary, and $P(\mathbf{x})$ is the normalized probability that a photon injected at some point on the boundary will have moved a transverse distance $\mathbf{x}$ along the boundary before exiting. Since the scattering angle θ is always very small, the integral in Eq. (1) is taken as two dimensional. This does not imply, of course, that the photon's random walk starts and ends on the boundary, and Eq. (1) is also correct for continuous injection, as well as for any other reasonable model for optical transport. Following Lagendijk, Vreeker, and De Vries,[26] we will neglect the dependence of $P(\mathbf{x})$ on the angle of incidence. This approximation is not only a good one, but is also not easily relaxed, since its abandonment would require the use of transport theory rather than diffusion theory, as well as the use of an anisotropic surface characterized by various unknown parameters which could not be easily obtained from experiment.

From the point of view of Eq. (1), the mechanism whereby the photon is displaced by $\mathbf{x}$ is quite irrelevant, so that normal photon diffusion, multiple reflections interspersed with normal diffusion, or any other physically reasonable set of processes are all covered equally well. Far above the optical Anderson transition[28,29] where $kl^*\gg 1$ (l^* is transport mean free path), the various photon paths may all be considered to be statistically independent. The same is also obviously true for successive passes of the light through the medium, so that the probabilities for these are simply additive, and $P(\mathbf{x})$, which appear in Eq. (1), is a simple sum over all the different ways in which a photon injected at the origin can exit at $\mathbf{x}$.

Our model of the optical transport is thus the following: A photon injected at the origin undergoes normal diffusion and may exit at $\mathbf{x}$. The probability for this is $t_sP_1(\mathbf{x})$, where t_s is the surface intensity transmission coefficient, and the superscript 1 denotes the fact that the photon has passed once through the random medium. $P_1(\mathbf{x})$ is the usual normalized probability density that is used in Eq. (1) to treat the coherent backscattering in the absence of surface reflections. Since each step in the random walk is independent not only of the previous step but also of the succeeding one, the "decision" of a photon at the last scattering event to head towards the boundary, which is considered to lie just outside the line of scatterers, is unaffected by the reflectivity of the boundary. Thus, reflection at the boundary corresponds to an independent reinjection of the photon, which then proceeds to execute a second, independent, random walk. As the sample albedo is assumed to be unity, all the light reflected back into the medium ultimately reappears at the boundary. Denoting the fraction of the incident light that the boundary reflects back into the medium by r, the probability that the photon will exit at $\mathbf{x}$ after one intermediate reflection (two passes through the medium) is $t_srP_2(\mathbf{x})$, where

$$P_{n+1}(\mathbf{x})=\int P_n(\mathbf{x}')P_1(\mathbf{x}-\mathbf{x}')d^2x' \ . \tag{2}$$

Summing all such processes, we have

$$P(\mathbf{x})=Nt_s(P_1+rP_2+r^2P_3+\cdots) \ ,$$

where the constant N is chosen such that $P(\mathbf{x})$ is normalized to unity, and is easily seen to be $N=(1-r)/t_s$. Since normalization always eliminates t_s from our final results, in what follows we simply omit this factor. Denoting the characteristic function of $P(\mathbf{x})$ (its Fourier transform) by $M(\mathbf{q})$, we have $M_{n+1}=M_nM_1=(M_1)^{n+1}$, so that we may immediately write for γ,

$$\gamma=(1-r)M_1\sum_{n=0}^{\infty}(rM_1)^n=(1-r)\gamma_0/(1-r\gamma_0) \ , \tag{3}$$

where $\gamma_0=M_1$ is the usual coherent-backscattering peak shape function in the absence of reflection. We note that $M_n(0)=1$, so that the normalization factor $(1-r)$ could also have been obtained at the end of the calculation simply by requiring that $\gamma(0)=1$. We will find it convenient to normalize the remainder of our results in this way. We also note that the effects of absorption can easily be included by using the appropriate form for P_1, and multiplying r by the (now less than unity) albedo, thereby incorporating the fact that a reflected photon may be absorbed before it can return to the surface. Accordingly, in what follows we no longer explicitly discuss absorption.

In Fig. 1(a), we plot as a function of r the half width of the coherent-backscattering peak normalized by the half width for $r=0$. We assume continuous injection and use the form for γ_0 given by Akkermans, Wolf, and Maynard.[30] We note that the resulting curve is a *universal* one and well illustrates the major effects of the surface reflections, which is to drastically narrow the peak. Also shown are the results of Lagendijk, Vreeker, and De Vries[26] for two different choices of the boundary conditions, one appropriate to $r=0$, and the other appropriate to $r=1$. As expected, our results fall, for the most part, midway between these two.

In general, the surface reflectivities of the various samples used in most of the previous coherent-backscattering experiments[5-11] are unknown. For the studies that used polystyrene spheres in water,[5-7] however, there are two sources of reflection that may be estimated. The first is total internal reflection at the external glass-air surface of the sample cell. For this $r=0.75$, leading to a drastic threefold reduction in peak width. This reflection can be effectively masked out in a properly designed cell, and, assuming that this has been done, a much smaller, intrinsic reflection still remains. This is the Fresnel reflection at the internal water-glass interface, which may be estimated to yield $r=0.12$. This leads to a 10% reduction in peak width. Accordingly, surface reflection effects can range from small (but not negligible) to very large, depending upon experimental conditions and so must be carefully considered in all future experiments. We recall the well-known effect that a matte surface can become highly reflecting at near grazing incidence, so that most samples will have a significant reflectivity which may prove difficult to characterize experimentally. Under some circumstances, index matching techniques[1] can be used to minimize these reflection effects.

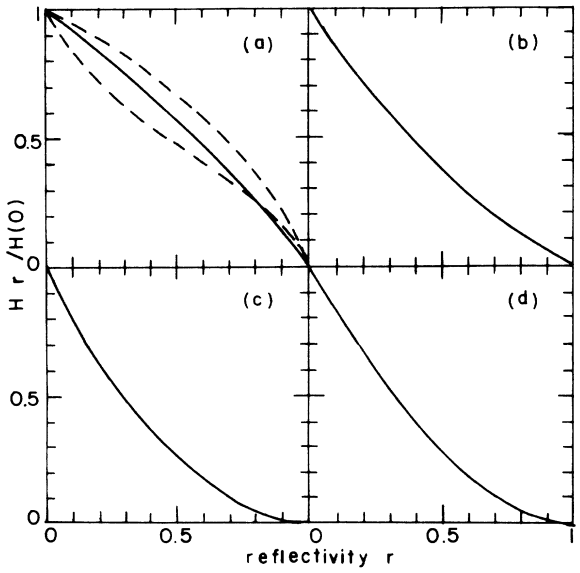

FIG. 1. Half width $H(r)$ for arbitrary effective surface reflectivity r normalized by $H(0)$ for reflection from an infinite half-space. (a) Coherent backscattering peak. (b) Optical memory effect form factor. (c) Frequency-dependent intensity correlation function. (d) Time-dependent dynamic intensity correlation function. These curves are all universal. In (a) the two dashed curves are obtained from the results of Ref. 26 for two different values of the diffusion equation boundary conditions. The upper dashed curve is for boundary conditions appropriate to $r=0$, while the lower dashed curve is for those appropriate to $r=1$.

B. One boundary—the optical memory effect

The form factor F for the optical memory effect[1-4] in reflection is simply related to the square of the coherent-backscattering peak,[1] i.e., $F=\gamma^2$, and $F_0=\gamma_0^2$, where F_0 is the form factor for $r=0$. Accordingly, we have

$$F=(1-r)^2F_0/(1-r\sqrt{F_0})^2 . \tag{4}$$

In Fig. 1(b), we plot the normalized half width of the form factor versus r. Also this curve is universal. As may be seen, F falls rapidly with r, and, for $r=0.75$, the half width of F is $\frac{1}{6}$ its value for $r=0$. There are currently no experiments that may be compared with Eq. (4), since available data are for the finite-thickness slab.[1]

C. One boundary—frequency-dependent correlations

The electric field–electric field frequency-dependent correlation function

$$C^e(\Omega)=\langle E(\omega)E^*(\omega+\Omega)\rangle$$

is related to the pulse-shape propagation function $I(t)$ by

$$I(t)=\left|\int e^{i\omega t}E(\omega)d\omega\right|^2$$
$$=\int e^{i\Omega t}\langle E(\omega)E^*(\omega+\Omega)\rangle d\Omega ,$$

where $I(t)$ is the time-dependent intensity at the output of the medium for a δ function input. Inverting the transform, we have that C^e is the characteristic function of I, i.e.,

$$C^e(\Omega)=\int e^{-i\Omega t}I(t)dt . \tag{5}$$

This is a very general, system-independent result. Under the assumption of statistically independent photon paths, the intensity-intensity frequency-dependent correlation function C^i is related to C^e by

$$C^i(\Omega)=\langle I(\omega)I(\omega+\Omega)\rangle-\langle I(\omega)\rangle\langle I(\omega+\Omega)\rangle$$
$$=|C^e(\Omega)|^2 .$$

Both $C^e(\Omega)$ and $C^i(\Omega)$ are normalized to unity at $\Omega=0$, since it is assumed that $\int I(t)dt=1$. We have also implicitly assumed that C^e is not sensitive to the particular value of ω (basic laser frequency) and that $\Omega/\omega\ll 1$. The foregoing has also been derived in a model-dependent fashion by Edrei and Kaveh[15] and by Genack and Drake.[31]

In analogy with our discussion of the coherent-backscattering peak, $I(t)$ in the presence of surface reflections can be written as

$$I(t)=N(I_1+rI_2+r^2I_3+\cdots) ,$$

where I_1 is the pulse shape obtained after one pass, i.e., no surface reflections, N is a normalization constant, and the pulse shape after $n+1$ passes is

$$I_{n+1}(t)=\int I_n(t')I_1(t-t')dt' . \quad (6)$$

Writing C_0^e for the (known) electric field correlation function in the absence of surface reflections, we immediately obtain

$$C^e=(1-r)C_0^e/(1-rC_0^e) . \quad (7)$$

We note that because $I(t)$ is asymmetric, $C^e(\Omega)$ is generally complex. Experimentally,[12] one measures the intensity correlation $C^i(\Omega)$, rather than $C^e(\Omega)$, and in order to compute C^i in terms of its value in the absence of reflection, C_0^i, the phase $\phi(\Omega)$ of C_0^e must be known. In terms of this, we have

$$C^i=(1-r)^2C_0^i/[1+r^2C_0^i-2r(C_0^i)^{1/2}\cos(\phi-\phi_0)] , \quad (8)$$

where both C_0^e and C_0^i are assumed normalized such that $C_0^e(0)=C_0^i(0)=1$, and $\phi_0=\phi(0)$.

For an infinite half space, Edrei and Kaveh[15] have obtained

$$C_0^i(x)=e^{-2x} ,$$

where

$$x=(1+\Delta)(6kl^*\Omega/\omega)^{1/2} ,$$

and $\Delta=0.7104$ from the boundary conditions of the diffusion equation.[27] Extending the calculation to include the phase ϕ, we find $\phi(x)-\phi_0=x$.

In Fig. 1(c), we plot the normalized half width of C^i versus r, where once again a rapid decrease of the half width with increasing r is evident. We note that also this curve is a universal one.

The experiments of Genack[15] were performed on fine rutile particles embedded in a polystyrene matrix with polished surfaces. For this system r may be estimated to be $r=0.9$ if the polished sample surface is reflecting. For such a high reflectivity, Eq. (8) predicts that the half width of the correlation function will be reduced to a mere 1% of its value in the absence of surface reflections. Lagendijk, Vreeker, and De Vries[26] have estimated that such a high reflectivity will broaden the reflected pulse shape by a less dramatic, but still very substantial factor of 3. We must note, however, that for transmission through thick samples, which corresponds to the experiments,[15] the effects of surface reflections are much less important but may still prove significant depending upon experimental parameters.

D. One boundary — time correlations

In a system of moving particles, the scattered electric field $E(t)$ fluctuates randomly with time. The spectral density $I(\Omega)$ is given by

$$I(\Omega)=\int e^{i\Omega t}\langle E(0)E^*(t)\rangle dt .$$

Inverting the transform, we have for the dynamic electric field correlation function

$$\langle E(0)E^*(t)\rangle=\int e^{-i\Omega t}I(\Omega)d\Omega .$$

We note that for randomly moving particles and the small frequency shifts Ω which are relevant here, the frequency spectrum of the scattered light is broadened symmetrically around ω_0, the frequency of the incident monochromatic laser beam, so that $I(\Omega)=I(-\Omega)$ and the dynamic electric field correlation function is both symmetric and real. Reinjecting the broadened spectrum into the medium leads to additional symmetric spectral broadening. Since each spectral component is independent of all the others, as are all the passes through the medium, we have for $I_{n+1}(\Omega)$,

$$I_{n+1}(\Omega)=\int I_n(\Omega')I_1(\Omega-\Omega')d\Omega' . \quad (9)$$

Writing

$$I(\Omega)=N(I_1+rI_2+r^2I_3+\cdots) ,$$

where N is a normalization constant, denoting the intensity-intensity time-dependent correlation function in the presence of surface reflections by $C(t)$, and the corresponding function in the absence of these reflections by $C_0(t)$, and again using the fact that for independent photon paths the intensity correlation function is the square of the (real) electric field correlation function, we have

$$C=(1-r)^2C_0/(1-r\sqrt{C_0})^2 , \quad (10)$$

where we have assumed that C_0 is normalized such that $C_0(0)=1$.

We might note that exactly the same calculation is implied by Eq. (9) gives C_0 itself, when we consider the successive frequency broadenings of the scattered light after each scattering event. In this case, of course, the relative weights of the different "passes" (i.e., orders of scattering) are not r^n, but may be denoted by W_n, while for a single-scattering event

$$\langle E(0)E^*(t)\rangle=\exp(-t/2\langle t_1\rangle) ,$$

where the average single-scattering correlation time $\langle t_1\rangle$ is determined by the particle diffusion constant. In this simple way we immediately recover Eq. (5) of Rosenbluh *et al.*[18] for C_0.

Using the compact form

$$C_0=\exp[-(1+\Delta)\sqrt{6t/\langle t_1\rangle}]$$

given by Pine *et al.*,[21] we plot in Fig. 1(d) the normalized half width of the intensity correlation function $C(t)$ versus r. Also this curve is universal, and displays the familiar rapid decrease with r. All the dynamic reflection experiments published to date[16–18,21,24] involve polystyrene spheres in water for which, as already discussed, the minimum possible value of the reflectivity is $r=0.12$. Accordingly, for all these experiments the observed half width is at least 20% too narrow, while further substantial narrowing is possible if the data are contaminated by additional reflections from the cell windows. Clearly, the effects of surface reflections must be considered in all future careful work.

E. Two boundaries—the finite thickness slab

As is now apparent, the success of our method depends upon the fact that for each process considered there is an underlying quantity, say $P(\mathbf{x})$, which is convoluted upon reinjection, while the process itself involves the Fourier transform of this convolution. This leads to the simple summations over all powers of the basic transform, say $M_1(\mathbf{q})$, which represents our final answer. Accordingly, we no longer write out the underlying convolutions, but instead work directly with the basic transforms. For the infinite half-space there was only one basic transform, corresponding to a single pass through the medium in which the photon returns to the input surface. Here we denote the corresponding transform for the slab by M_R. We note that M_R depends, of course, upon the slab thickness L. The second basic transform for the slab corresponds to a single pass through the medium in which the photon arrives at the second surface. We denote this transform by M_T.

These two basic transforms correspond to different quantities for the different processes. In the absence of surface reflections, the coherent-backscattering peak shape is $M_R(\mathbf{q})$, the memory effect form factor in reflection is $M_R^2(\mathbf{q})$, and in transmission $M_T^2(\mathbf{q})$, the electric field frequency correlation function in reflection is $M_R(\Omega)$, and in transmission $M_T(\Omega)$, while the dynamic electric field correlation function is $M_R(t)$ in reflection, and $M_T(t)$ in transmission. We recall that the intensity correlation functions are the squares of the corresponding electric field correlation functions. As before, we assume that $M_R(0)=M_T(0)=1$. In most instances, both M_R and M_T are available for the finite slab without surface reflections in one or more of the references already cited.[2–25] The one important exception to this is the phase of the frequency-dependent electric field correlation function, which does not appear to have been given explicitly before. The total transforms which include all the internal multiple reflections and transmissions we denote by $\mathcal{R}$ for reflection and $\mathcal{T}$ for transmission. These are related to the various processes already listed above, coherent-backscattering peak, correlation functions, etc., in the same way as are the corresponding M_R and M_T. $\mathcal{R}$ and $\mathcal{T}$ are also normalized such that $\mathcal{R}(0)=\mathcal{T}(0)=1$.

We label the initial input surface by 1, the second surface of the slab by 2, and assume generally different reflectivities r_1 and r_2 for these two surfaces. In Fig. 2(a) we display the six different elementary diagrams we will need. As shown in the figure, R corresponds to direct injection of the incident light at surface 1 followed by a random walk which returns to the same surface. For the finite slab the albedo is no longer unity, but rather $1-t_D$, where t_D is the diffuse transmittance of the slab. Accordingly, we have $R=(1-t_D)M_R$. T corresponds to direct injection of the incident light at surface 1 followed by a random walk which reaches surface 2. Accordingly, $T=t_D M_T$. R_1 corresponds to reinjection of the light at surface 1 due to a surface reflection which is then followed by a random walk which returns to the same surface, so $R_1=r_1 R$. T_1 corresponds to reinjection of the light at surface 1 due to a surface reflection followed by a random walk which reaches surface 2. Accordingly we have $T_1=r_1 T$. In a similar fashion, we have $R_2=r_2 R$, and $T_2=r_2 T$.

In Figs. 2(b)–2(d) we combine these elementary diagrams so as to describe the total random walk. There are, of course, various ways of doing this, but we believe that the combinations we have chosen lead to the simplest method of calculation. In Fig. 2(b) we show the two different ways of starting the random walk. We label these by S_{11} and S_{12}, where the first subscript indicates the initial surface, and the second subscript the final surface. In Fig. 2(c) we show the two different ways in which the random walk may continue, and in Fig. 2(d) we show the four different ways in which it may end. In these diagrams, a dashed line corresponds to a process which may be repeated an arbitrary number of times. In terms of the elementary diagrams of Fig. 2(a), we have

$$S_{11}=R, S_{12}=T \ , \tag{11a}$$

$$C_{11}=\left[\sum_{n=0}^{\infty} R_1^n\right] T_1 \left[\sum_{m=0}^{\infty} R_2^m\right] T_2 = T_1 T_2/(1-R_1)(1-R_2) \ , \tag{11b}$$

$$C_{22}=C_{11}=C \ , \tag{11c}$$

$$E_{11}=1/(1-R_1), \ E_{21}=T_2/(1-R_1)(1-R_2) \ , \tag{11d}$$

$$E_{12}=T_1/(1-R_1)(1-R_2), \ E_{22}=1/(1-R_2) \ . \tag{11e}$$

Note that C is bounded by $0\le C\le 1$. The lower limit is reached when any of the quantities r_1, r_2, or t_D vanish, while the upper limit is reached when $r_1=r_2=1$. Since C itself may be repeated any arbitrary number of times, we have

$$\mathcal{R}=N_R\left[S_{11}\left[\sum_{n=0}^{\infty} C_{11}^n\right]E_{11}+S_{12}\left[\sum_{m=0}^{\infty} C_{22}^m\right]E_{21}\right] \ , \tag{12a}$$

$$\mathcal{T}=N_T\left[S_{11}\left[\sum_{n=0}^{\infty} C_{11}^n\right]E_{12}+S_{12}\left[\sum_{m=0}^{\infty} C_{22}^m\right]E_{22}\right] \ , \tag{12b}$$

where N_R and N_T are normalization constants. Defining

$$D=(1-R_1)(1-R_2)-T_1T_2 \ , \tag{13a}$$

and

$$N=(1-r_1r_2t_D)-(1-t_D)(r_1+r_2-r_1r_2) \ , \tag{13b}$$

we have

$$\mathcal{R}=N_R[R(1-R_2)+T_2]/D \ , \tag{14a}$$

$$N_R=N/[(1-t_D)(1-r_2)+r_2t_D] \ , \tag{14b}$$

and

$$\mathcal{T}=N_T T/D \ , \tag{15a}$$

$$N_T=N/t_D \ . \tag{15b}$$

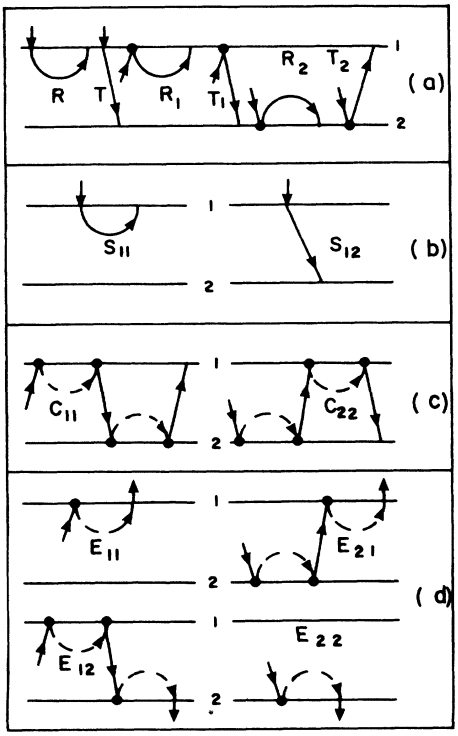

FIG. 2. Diagrams used in the calculations for the finite thickness slab. (a) Elementary diagrams. (b) Start of random walk. (c) Continuation of random walk. (d) End of random walk. A dashed line corresponds to a process that may be repeated an arbitrary number of times, while a large dot corresponds to an internal surface reflection. The values of the various diagrams are listed in the text.

It is straightforward to verify that $\mathcal{R}$ and $\mathcal{T}$ both pass to the proper limiting forms for various combinations of the parameters r_1, r_2, and t_D going to either zero or to unity.

F. Two boundaries—diffuse reflections and transmittance

Our calculations have assumed that the intensity of the injected light is unity, so that the sum of the total diffuse reflectance ρ and the total diffuse transmittance τ is $\rho+\tau=1$. In a real experimental situation, there may be some true specular reflection of the incident beam which reduces the injected intensity. As is well known, if the refractive index is 1.5, this loss of intensity is only 4% for the case of normal incidence assumed here. We emphasize that r_1, for example, which may reach 0.75, is a result of integrating over *all* internal angles, and is thus very much greater than this 4% specular reflection for normal incidence. In a comparison of experiment with theory for the special case of very high index media with smooth surfaces which have a high reflectance at normal incidence, it may be necessary to multiply both ρ and τ by the normal incidence surface transmittance. In general, however, for matte surfaces and moderate refractive indices, no such correction will be required.

The diffuse reflectance or transmittance is obtained by summing all the reflected or transmitted intensities and then multiplying by the surface transmission coefficient, which is $1-r_1$ for reflection, and $1-r_2$ for transmission. We thus obtain

$$\rho=(1-r_1)/N_R \ , \tag{16a}$$

$$\tau=(1-r_2)/N_T \ . \tag{16b}$$

It is easily verified that ρ and τ indeed sum to unity, and that they pass to the proper limiting values for various special cases, including the interesting limit $r_1=r_2=1$, where $\rho=\tau=\frac{1}{2}$. We note that the effects of internal surface reflections generally make τ greater than t_D. This may be easily seen by considering the special case of $r_1=r_2=r$, for which

$$\tau/t_D=[1-r(1-2rt_D)]^{-1} \ ,$$

which exceeds unity when $t_D<\frac{1}{2}$, as is usually the case. For $r=0.75$ and $t_D=0.1$, for example, $\tau/t_D=2.8$. (The general rule is that the reflections tend to move both ρ and τ towards their limiting values of $\frac{1}{2}$.) Since the measured diffuse transmittance may be used to estimate the transport mean free path l^*, erroneously large results for this latter quantity can be obtained if the effects of surface reflections are neglected.

III. COMPARISON WITH EXPERIMENT

The only available quantitative data which appears suitable for comparison with our theoretical expressions are the very recent results by Freund, Rosenbluh, and Berkovits on the optical memory effect.[1] Using index matching techniques, these authors showed that for some samples internal surface reflections played a dominant role in determining the width and shape of the memory effect form factors for both reflection and transmission. These samples were composed of a dilute concentration of fine rutile particles in a polystyrene matrix which took the form of a thin slab. Although the slab surfaces appeared matte for near normal incidence, at smaller glancing angles the surfaces became reflecting. Accordingly, we can expect that above the critical angle total internal reflection occurs, leading to $r_1=r_2=0.78$. Since the slab thickness L is known, the only undetermined parameter is the transport mean free path l^*. We obtain this by matching the theory to the experiments in reflection, where the form factor is sensitive to l^*, and we then use this value to compare theory with experiment for transmission. We emphasize that in making this latter comparison there are no longer any adjustable parameters.

Writing $y=qL$, the two basic transforms we require may be written[2-4]

$$M_T=y/\sinh(y) \ , \tag{17a}$$

$$M_R=\sinh(yt_D)\sinh[y(1-t_D)]/[yt_D(1-t_D)\sinh(y)] \ , \tag{17b}$$

where in view of the various approximations already present in these form factors (diffusion theory, point, rather than continuous injection, $\Delta=0$, etc.), we have, for

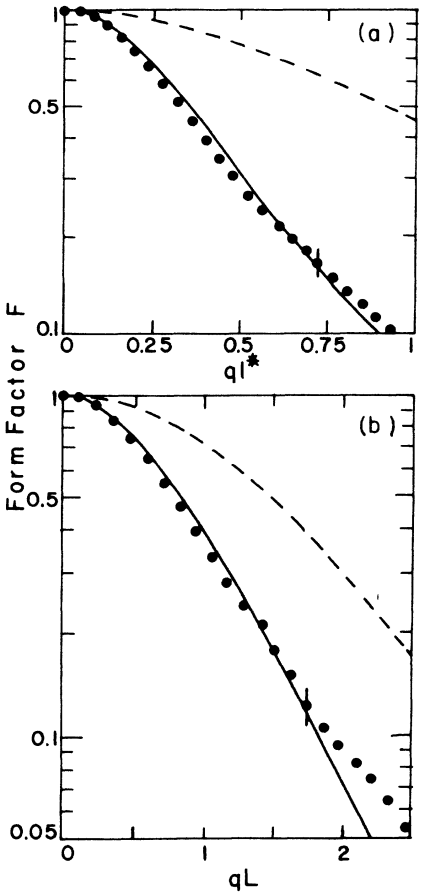

FIG. 3. Memory effect form factors for a thin slab in (a) reflection and (b) transmission. The data points are from Ref. 1. The solid curve in (a) is a fit to the theory which includes internal reflections, Eq. (14), as described in the text, while the dashed curve is the theory without reflections. In (b) there are no adjustable parameters, and the solid curve includes internal reflections, Eq. (15), while the dashed curve neglects these.

simplicity, set $t_D = l^*/L$. The results of the analysis are displayed in Fig. 3. In Fig. 3(a), we show the match between theory and experiment for $t_D = 0.38$ as the solid curve, while the broken curve is the theoretical result in the absence of internal surface reflections. The dominant role of these reflections is strikingly evident. Using the above value of t_D, we plot in Fig. 3(b) a comparison between theory and experiment for the case of transmission. As before, the solid curve includes the effects of the internal surface reflections, while the dashed curve is the theory without these. The internal reflections are readily seen to be important here also. We note that the substantial level of agreement between the theory which includes these reflections and the experiments is obtained with no adjustable parameters, so that this agreement provides a significant verification of the theory.

IV. SUMMARY

We have presented simple, closed-form expressions for a finite-thickness slab with arbitrary surface reflections for a wide variety of phenomena in both reflection and transmission. These phenomena include the shape of the coherent-backscattering peak, the form factors of the optical memory effect, the frequency-dependent correlation functions for static systems, the time-dependent correlation functions for dynamic systems, and the diffuse reflectance and transmittance. A major advantage of the approach we have used is that it permits retention of a substantial body of prior theory, since we have shown how to express the effects of internal reflection in terms of the results already obtained in the absence of these reflections. In every instance we have found that the effects of internal surface reflections are significant, and in some cases dominant. We have applied the theory to available data on the optical memory effect and found good agreement with experiment. The results presented here together with the important prior results of Lagendijk and coworkers,[26] make it abundantly clear that internal surface reflections need to be considered in almost all theoretical and experimental work on optical transport in random media. We note that in the propagation of various other kinds of waves through random media, such as sound waves or electron waves, important impedance mismatches at sample boundaries may also occur and result in significant internal reflections. We suggest that the methods developed here may prove useful also for these systems.

ACKNOWLEDGMENTS

We are pleased to acknowledge the support of the Israel Academy of Sciences and Humanities, and the U.S.-Israel Binational Science Foundation (BSF), Jerusalem.

[1] I. Freund, M. Rosenbluh, and R. Berkovits, Phys. Rev. B **39**, 12 403 (1989).
[2] S. Feng, C. Kane, P. A. Lee, and A. D. Stone, Phys. Rev. Lett. **61**, 834 (1988).
[3] I. Freund, M. Rosenbluh, and S. Feng, Phys. Rev. Lett. **61**, 2328 (1988).
[4] R. Berkovits, M. Kaveh, and S. Feng, Phys. Rev. B **40**, 737 (1989).
[5] Y. Kuga and A. Ishimaru, J. Opt. Soc. Am. A **1**, 831 (1984); L. Tsang and A. Ishimaru, *ibid.* **2**, 2187 (1985).
[6] M. P. van Albada and A. Lagendijk, Phys. Rev. Lett. **55**, 2692 (1985).
[7] P. E. Wolf and G. Maret, Phys. Rev. Lett. **55**, 2696 (1985).
[8] S. Etemad, R. Thompson, and M. J. Andrejco, Phys. Rev. Lett. **57**, 575 (1986).
[9] M. Kaveh, M. Rosenbluh, I. Edrei, and I. Freund, Phys. Rev. Lett. **57**, 2049 (1986).
[10] M. Rosenbluh, I. Edrei, M. Kaveh, and I. Freund, Phys. Rev. A **35**, 4458 (1987).
[11] I. Freund, M. Rosenbluh, R. Berkovits, and M. Kaveh, Phys. Rev. Lett. **61**, 1214 (1988).
[12] A. Z. Genack, Phys. Rev. Lett. **58**, 2042 (1987).

[13]B. Shapiro, Phys. Rev. Lett. **57**, 2168 (1986).
[14]M. J. Stephen and G. Cwillich, Phys. Rev. Lett. **59**, 285 (1987).
[15]I. Edrei and M. Kaveh, Phys. Rev. B **38**, 950 (1988).
[16]G. Maret and P. E. Wolf, Z. Phys. B **65**, 409 (1987).
[17]M. Kaveh, M. Rosenbluh, and I. Freund, Nature (London) **326**, 778 (1987).
[18]M. Rosenbluh, M. Hoshen, I. Freund, and M. Kaveh, Phys. Rev. Lett. **58**, 2754 (1987).
[19]M. J. Stephen, Phys. Rev. B **37**, 1 (1988).
[20]I. Freund, M. Kaveh, and M. Rosenbluh, Phys. Rev. Lett. **60**, 1130 (1988).
[21]D. J. Pine, D. A. Weitz, P. M. Chaiken, and E. Herbolzheimer, Phys. Rev. Lett. **60**, 1134 (1988).
[22]A. J. Rimberg and R. M. Westervelt, Phys. Rev. B **38**, 5073 (1988).
[23]I. Edrei and I. Freund, Phys. Rev. B **39**, 9660 (1989).
[24]D. N. Qu and J. C. Dainty, Opt. Lett. **13**, 1066 (1988).
[25]I. Edrei and M. Kaveh, Phys. Rev. B **38**, 950 (1988).
[26]A. Lagendijk, R. Vreeker, and P. De Vries, Phys. Lett. A **136**, 81 (1989).
[27]P. M. Morse and H. Feschbach, *Methods of Theoretical Physics* (McGraw-Hill, New York, 1953).
[28]S. John, Phys. Rev. Lett. **53**, 2169 (1984).
[29]P. W. Anderson, Philos. Mag. B **52**, 505 (1985).
[30]E. Akkermans, P. E. Wolf, and R. Maynard, Phys. Rev. Lett. **56**, 1471 (1986).
[31]A. Z. Genack and J. M. Drake (unpublished).